Earing prediction of AA 2008-T4 with anisotropic Drucker yield function based on the second and third stress invariants

IOP Conf. Series: Journal of Physics: Conf. Series **1063** (2018) 012113 doi:10.1088/1742-6596/1063/1/012113

Earing prediction of AA 2008-T4 with anisotropic Drucker yield function based on the second and third stress invariants

Saijun Zhang[1,2], Yanshan Lou[2], Jeong Whan Yoon[2,3,*]

[1] School of Mechanical and Automotive Engineering, South China University of Technology, 381 Wushan Road, Tianhe District, Guangzhou 510640, China
[2] Institute for Frontier Materials, Deakin University, 75 Pigdons Road, Waurn Ponds, VIC 3216, Australia
[3] Department of Mechanical Engineering, KAIST, 291 Daehak-ro, Yuseong-gu, Daejeon 305-701, Republic of Korea

j.yoon@deakin.edu.au / j.yoon@kaist.ac.kr

Abstract. This paper applies anisotropic Drucker yield function [14] (Lou and Yoon, 2018, Int. J. Plasticity 101, 125-55) to predict earing profile after cup deep drawing of AA 2008-T4. The new yield function is implemented into ABAQUS/Explicit using semi-implicit integration algorithm to calculate the increment of plastic strain. Both associated and non-associated flow rules are incorporated in this study. The predicted anisotropy and cup height profile are compared with the experimental results and those predicted from the Hill48, Yld91 and Yld2004-18p yield functions. It is observed that the earing profile predicted from the new yield function shows high accuracy. The computation time is also compared to investigate the computation cost of different yield functions. The comparison reveals that it takes the shortest time for the Hill48 function, the anisotropic Drucker yield function reduces 30%～40% of computation cost compared with the Yld91 and Yld2004-18p functions. It is concluded from the simulation of cup deep drawing that the new yield function can provide high accurate numerical analysis of plastic deformation for anisotropic metals with competitive computation cost.

1. Introduction

Extensive research has proven that the accuracy and efficiency of the numerical prediction results are closely related to the constitutive models. Various anisotropic yield functions have been developed to describe the anisotropic behavior of sheet metals under associate flow rule (AFR) [1-8]. The directional *r*-values and yield stresses can also be described accurately under non-AFR [9,10]. Some of these anisotropic models have been implemented into the finite element codes and used for the earing prediction [11-13].

Recently, Lou and Yoon [14] proposed the anisotropic Drucker yield function based on the second and third stress invariants and reported that 60% reduction of computation cost can be achieved compared with the Yld2004-18p function. In this paper, the anisotropic Drucker yield function is applied to describe the anisotropic plastic behavior of AA 2008-T4. The earing profile is also predicted by the anisotropic Drucker yield function as well as the Hill48, Yld91 and Yld2004-18p functions and compared with experimental measurement for the evaluation of their accuracy. The computation time is

also compared to assess the computing efficiency of these yield functions in numerical simulation of metal forming.

2. The anisotropic Drucker yield function

The anisotropic Drucker yield function was developed by Lou and Yoon [14] to describe the anisotropic behavior of metals under spatial loading, which is in a form of

$$f(\sigma_{ij}) = \bar{\sigma} = \frac{1}{n}\sum_{m=1}^{n}\left\{\left[\left(J_2^{\prime(m)}\right)^3 - c\left(J_3^{\prime(m)}\right)^2\right]^{1/6}\right\} \tag{1}$$

In equation (1), $J_2^{\prime(m)}$ and $J_3^{\prime(m)}$ are functions of the linear transformed stress tensor $\mathbf{s}^{\prime(m)}$ given by

$$J_2^{\prime(m)} = -s_{11}^{\prime(m)}s_{22}^{\prime(m)} - s_{22}^{\prime(m)}s_{33}^{\prime(m)} - s_{11}^{\prime(m)}s_{33}^{\prime(m)} + \left(s_{12}^{\prime(m)}\right)^2 + \left(s_{23}^{\prime(m)}\right)^2 + \left(s_{13}^{\prime(m)}\right)^2 \tag{2}$$

$$J_3^{\prime(m)} = s_{11}^{\prime(m)}s_{22}^{\prime(m)}s_{33}^{\prime(m)} + 2s_{12}^{\prime(m)}s_{23}^{\prime(m)}s_{13}^{\prime(m)} - s_{11}^{\prime(m)}\left(s_{23}^{\prime(m)}\right)^2 - s_{22}^{\prime(m)}\left(s_{13}^{\prime(m)}\right)^2 - s_{33}^{\prime(m)}\left(s_{12}^{\prime(m)}\right)^2 \tag{3}$$

where $\mathbf{s}^{\prime(m)}$ is defined as

$$\mathbf{s}^{\prime(m)} = \mathbf{L}^{\prime(m)}\boldsymbol{\sigma} \tag{4}$$

with the fourth order linear transformation tensor $\mathbf{L}^{\prime(m)}$ in a form of

$$\mathbf{L}^{\prime(m)} = \begin{bmatrix} \left(c_2^{\prime(m)} + c_3^{\prime(m)}\right)/3 & -c_3^{\prime(m)}/3 & -c_2^{\prime(m)}/3 & 0 & 0 & 0 \\ -c_3^{\prime(m)}/3 & \left(c_3^{\prime(m)} + c_1^{\prime(m)}\right)/3 & -c_1^{\prime(m)}/3 & 0 & 0 & 0 \\ -c_2^{\prime(m)}/3 & -c_1^{\prime(m)}/3 & \left(c_1^{\prime(m)} + c_2^{\prime(m)}\right)/3 & 0 & 0 & 0 \\ 0 & 0 & 0 & c_4^{\prime(m)} & 0 & 0 \\ 0 & 0 & 0 & 0 & c_5^{\prime(m)} & 0 \\ 0 & 0 & 0 & 0 & 0 & c_6^{\prime(m)} \end{bmatrix} \tag{5}$$

In equation (1), the coefficient c is suggested to be 1.226 for BCC and 2 for FCC metals. Obviously, the anisotropic Drucker yield function reduces to the Hill48 yield function when $n = 1$ and $c = 0$.

3. Calibration of the anisotropic Drucker function

There are six anisotropic parameters for each component in the anisotropic Drucker yield function. Since the out-of-plane parameters, $c_4^{\prime(m)}$and $c_5^{\prime(m)}$, are suggested to be identical with $c_6^{\prime(m)}$, there are only four in-plane anisotropic parameters to be calibrated for each component. The anisotropic Drucker yield function is applied to describe the anisotropic behavior of AA 2008-T4 with experimental normalized yield stresses and *r*-values in Table 1. Considering that c is a constant, there are four parameters for $n = 1$ and eight parameters for $n = 2$ to be calibrated by the experimental data. For $n = 1$, the four anisotropic parameters are calibrated by r_0, r_{45}, r_{90} and σ_0, or, σ_0, σ_{45}, σ_{90} and σ_b. For $n = 2$, the eight anisotropic parameters are calibrated by r_0, r_{15}, r_{30}, r_{45}, r_{60}, r_{75}, r_{90} and σ_0 or σ_0, σ_{15}, σ_{30}, σ_{45}, σ_{60}, σ_{75}, σ_{90} and σ_b. The optimized anisotropic coefficients are tabulated in Table 2.

The directional yield stresses and *r*-values predicted by the anisotropic Drucker yield function are shown in Figures 1 and 2 for $n = 1$ and in Figure 3 for $n = 2$. The predicted results by popular yield functions, such as Hill48, Yld91 and Yld2004-18p which are calibrated with the same experimental data are also included in the figures for the comparison purpose. The theoretical directional yield stresses and *r*-values predicted from the anisotropic Drucker yield function are identical to that of Hill48 for $c = 0$ and are of negligible difference compared with that of Yld91 when $c = 2$ and $n = 1$. The anisotropic Drucker yield function for $c = 2$ and $n = 2$ calibrated from the directional *r*-values or yield stresses provides the same order of accuracy as obtained by the Yld2004-18p function, as shown in Figure 3. The yield locus of the anisotropic Drucker yield function for $n = 1$ and $n = 2$ is compared in Figure 4 and Figure 5, respectively. The comparison with experimental results shows that the anisotropic Drucker function can capture both directional yield stresses and *r*-values of AA 2008-T4 with high accuracy.

Table 1. Normalized yield stresses and *r*-values of AA 2008-T4

yield stress	σ_0/σ_0	σ_{15}/σ_0	σ_{30}/σ_0	σ_{45}/σ_0	σ_{60}/σ_0	σ_{75}/σ_0	σ_{90}/σ_0	σ_b/σ_0
	1.000	0.9963	0.9835	0.9459	0.9303	0.9171	0.9044	0.9010
r-values	r_0	r_{15}	r_{30}	r_{45}	r_{60}	r_{75}	r_{90}	r_b
	0.8674	0.8077	0.6188	0.4915	0.4955	0.5114	0.5313	–

Table 2. Calibrated parameters of anisotropic Drucker functions for AA 2008-T4

	$c_1'^{(1)}$	$c_2'^{(1)}$	$c_3'^{(1)}$	$c_6'^{(1)}$	$c_1'^{(2)}$	$c_2'^{(2)}$	$c_3'^{(2)}$	$c_6'^{(2)}$	c	n
Drucker1n-r	2.3147	1.7871	1.6765	1.6720					0	1
Drucker1n-σ	2.0996	1.7395	1.7246	1.7997					0	1
Drucker1n-r	2.1913	1.8729	1.7995	1.7829					2	1
Drucker1n-σ	2.2190	1.8448	1.8282	1.9083					2	1
Drucker2n-r	3.4948	2.8308	3.5130	3.3386	1.5433	0.7778	0.0367	-0.1034	2	2
Drucker2n-σ	2.3007	2.5455	-3.7739	1.8589	2.0831	1.1176	2.1676	-1.8779	2	2

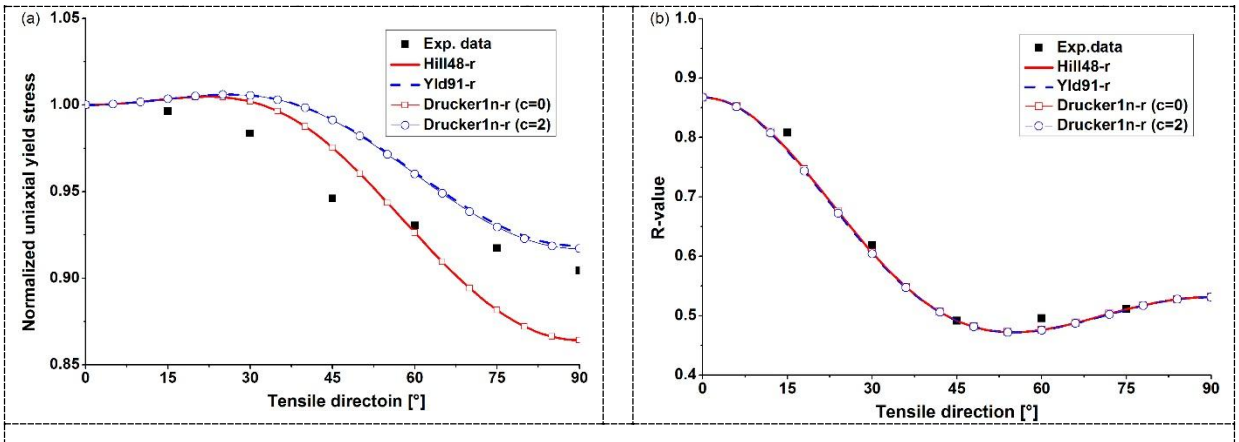

Figure 1. Comparison of AA 2008-T4 predicted by the anisotropic Drucker yield function ($n = 1$) calibrated by r_0, r_{45}, r_{90} and σ_0: (a) uniaxial tensile yield stress; (b) *r*-values.

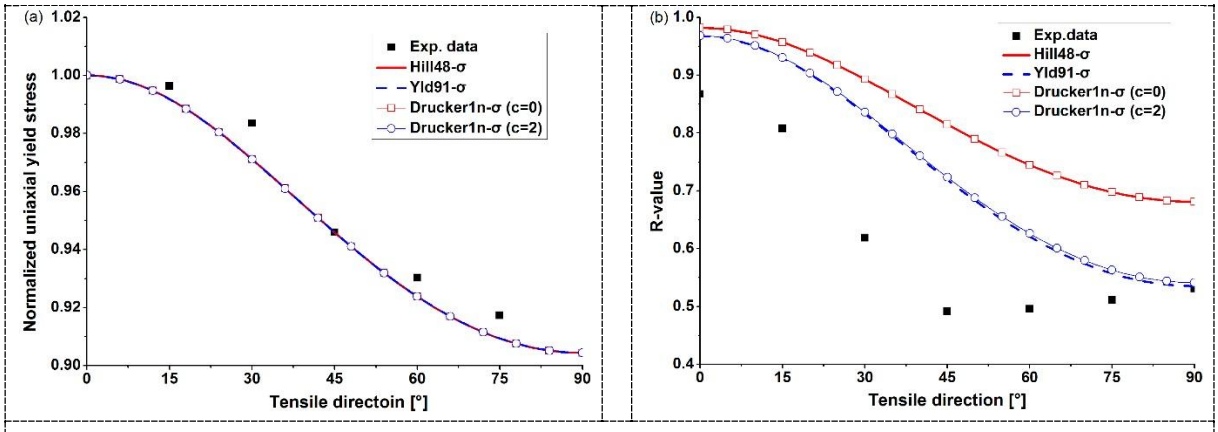

Figure 2. Comparison of AA 2008-T4 predicted by the anisotropic Drucker yield function ($n = 1$) calibrated by σ_0, σ_{45}, σ_{90} and σ_b: (a) uniaxial tensile yield stress; (b) *r*-values.

4. Earing prediction of AA 2008-T4

The numerical simulation of the cup drawing test of AA 2008-T4 is carried out to evaluate the performance of the anisotropic Drucker function. The dimensions of the tools and the process variables used in the simulations are given in [11]. Taking the advantage of axis symmetry of the model, only a quarter section of the cup is analyzed with enforced symmetric boundary conditions. 3D solid elements are employed in finite element modeling of cup deep drawing. Semi-implicit integration algorithm is used to calculate the increment of plastic strain.

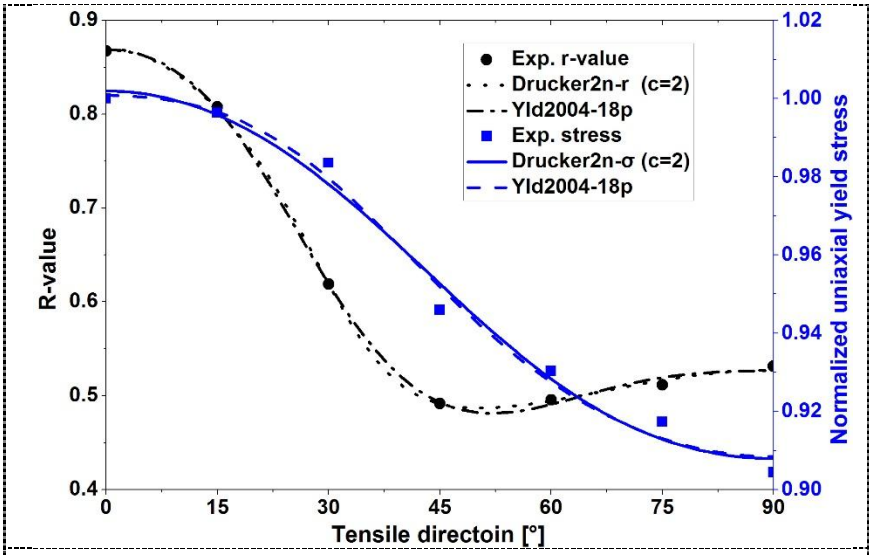

Figure 3. Comparison of AA 2008-T4 predicted by the anisotropic Drucker yield function ($n = 2$) calibrated by directional *r*-values and yield stresses.

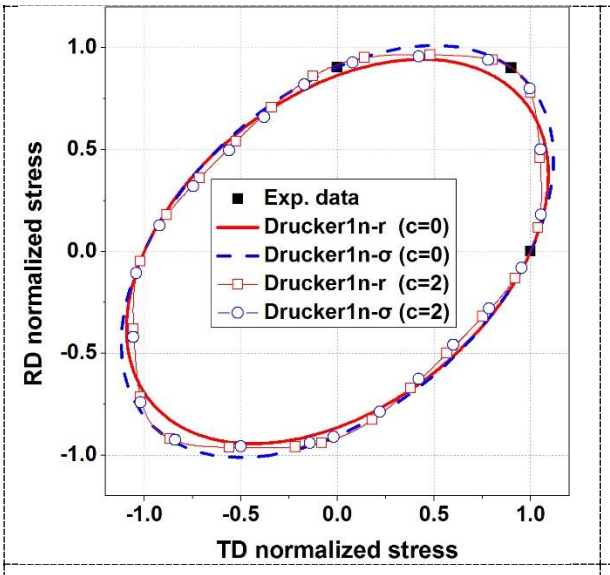

Figure 4. Comparison of yield locus of the anisotropic Drucker yield function ($n = 1$).

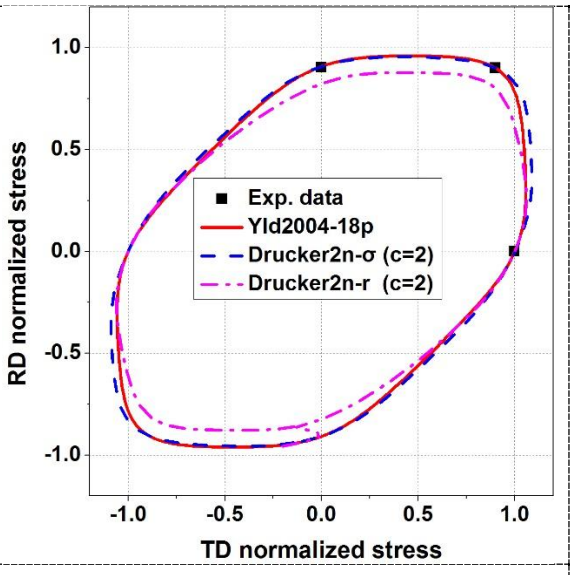

Figure 5. Comparison of yield locus of the anisotropic Drucker yield function ($n = 2$).

The earing profiles predicted from the anisotropic Drucker yield function for $n = 1$ are compared with the measured ear profiles, as shown in Figure 6. The results using the Hill48 and Yld91 yield functions are also included in Figure 6 for the comparison purpose. It is observed that the earing profile predicted from the anisotropic Drucker yield function is identical as that of Hill48 for $c = 0$ and is identical to that of Yld91 when $c = 2$ and $n = 1$. Although the earing trend is well predicted by all the models, the difference in cup height predicted by the anisotropic Drucker yield function for $c = 2$ is lower than that for $c = 0$. It may be because the anisotropy of the directional yield stress in Figure 1(a) is overestimated for $c = 0$.

The ear profiles predicted from the anisotropic Drucker yield function under non-associated flow rule (non-AFR) are also evaluated, as shown in Figure 7. The results using the Hill48 and Yld91 functions under non-AFR and using Yld2004-18p under AFR are also included in Figure 7 for the comparison purpose. The comparison shows that the anisotropic Drucker function under non-AFR with $n = 1$ and $c = 2$ predicts the same ear profile as that predicted by Yld91 under non-AFR, and both models underestimate the cup height difference compared with that predicted by Yld2004-18p under AFR. Although both models predict more reasonable ear profile, the cup height difference predicted from the anisotropic Drucker function with $n = 2$ and $c = 2$ under non-AFR is higher than that predicted from the Hill48 function under non-AFR.

The computation time of the numerical simulations for these models is compared in Table 3. It is obvious that it takes the shortest time for the Hill48 function. Although the anisotropic Drucker function when $n = 1$ and $c = 2$ predicts the same results with the Yld91 function, the former improves the computation efficiency of about 30%～40%. The anisotropic Drucker function with $n = 2$ and $c = 2$ under non-AFR reduce the computation time of about 40% compared with the Yld2004-18p function. Lou and Yoon [14] reported that the anisotropic Drucker yield function reduces 60% of computation cost compared with the Yld2004-18p function. This is because the example shown in Lou and Yoon [14] is a nonlinear problem without involving any contact. The comparison shows that the anisotropic Drucker function provides high accuracy in numerical analysis with competitive computation cost.

5. Conclusions

The newly proposed anisotropic Drucker function is implemented into ABAQUS/Explicit using semi-implicit integration algorithm to predict earing profile of cup deep drawing of AA 2008-T4. It is observed that the earing trend is well predicted from the anisotropic Drucker yield function. The ear profile predicted by the anisotropic Drucker yield function is the same as that of Hill48 in case of $c = 0$ and is identical to that of Yld91 when $c = 2$ and $n = 1$. The comparison of computation time reveals that it takes the shortest time for the Hill48 function, and that the anisotropic Drucker yield function improves the computational efficiency of 30%～40% compared with the Yld91 and Yld2004-18p functions. The comparison shows that the anisotropic Drucker function provides high accuracy in numerical analysis with competitive computation cost.

Acknowledgments

The authors would like to thank the Guangdong National Natural Science Foundation under Grant Nos. 2016A030313453 and 2016A030313519, for their supports of this study. Supports from the ARC linkage project: LP150101027 are also highly acknowledged.

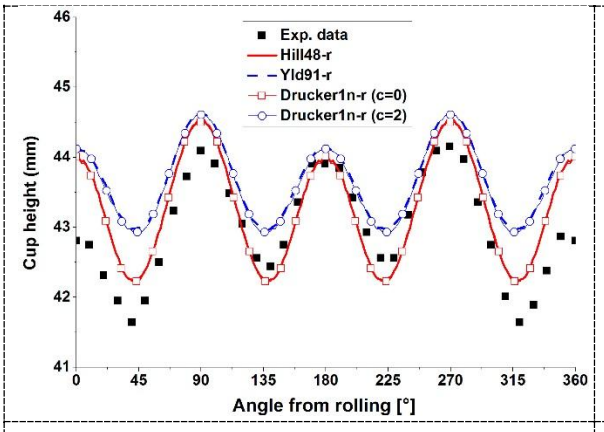

Figure 6. Earing profile predicted from the anisotropic Drucker function under AFR ($n = 1$).

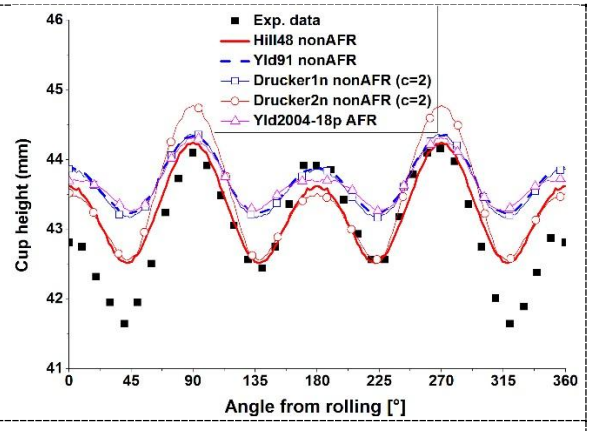

Figure 7. Earing profile predicted from the anisotropic Drucker function under non-AFR.

Table 3. Comparison of computational cost for different anisotropic functions

Software	Abaqus 6.14-4 Explicit/Double Precision/2 Cpus		
System	64-bit operating system		
Processor	Intel(R) Core(TM) i5-2430M CPU@2.40GHz		
Algorithm	Semi-implicit stress integration		
Computation time	Hill48-r	01:05:05	1.00
	Hill48-(non-AFR)	01:07:20	1.03
	Yld91-r	01:51:05	1.71
	Yld91-(non-AFR)	02:42:35	2.50
	Drucker1n-r (c=2)	01:22:19	1.26
	Drucker1n-(non-AFR, c=2)	01:55:26	1.77
	Drucker2n-r (c=2)	01:41:25	1.56
	Drucker2n-(non-AFR, c=2)	02:15:34	2.08
	Yld2004-18p	03:38:37	3.36

References

[1] Hill R 1948 *Proc. R. Soc. Lond.* **A193** 281-97
[2] Barlat F, Lege DJ, Brem JC 1991 *Int. J. Plasticity* **7** 693-712
[3] Barlat F, Brem JC, Yoon JW, Chung K, Dick RE, Lege DJ, Pourboghrat F, Choi SH, Chu E 2003 *Int. J. Plasticity* **19** 1297-319
[4] Barlat F, Aretz H, Yoon JW, Karabin ME, Brem JC, Dick RE 2005 *Int. J. Plasticity* **21** 1009-39
[5] Banabic D, Aretz H, Comsa DS, Paraianu L 2005 *Int. J. Plasticity* **21** 493-512
[6] Cazacu O, Barlat F 2001 *Math. Mech. Solids* **6** 613-30
[7] Lou Y, Huh H, Yoon JW 2013 *Int. J. Mech. Sci.* **66** 214-23
[8] Yoon JW, Lou Y, Yoon J, Glazoff MV 2014 *Int. J. Plasticity* **56** 184-202
[9] Stoughton TB 2002 *Int. J. Plasticity* **18** 687-714
[10] Stoughton TB, Yoon JW 2009 *Int. J. Plasticity* **25** 1777-817
[11] Chung K, Shah K 1992 *Int. J. Plasticity* **8** 453-76
[12] Yoon JW, Barlat F, Dick RE, Chung K, Kang TJ 2004 *Int. J. Plasticity* **20** 705-31
[13] Yoon JW, Barlat F, Dick RE, Karabin ME 2006 *Int. J. Plasticity* **22** 174-93
[14] Lou Y, Yoon JW 2018 *Int. J. Plasticity* **101** 125-55